[10]J. Krieger and M. Nightingale, Phys. Rev. B 4, 1266 (1971).
[11]S. Von Molnar and M. Shafer, J. Appl. Phys. 41, 1093 (1970).
[12]J. Axe, J. Phys. Chem. Solids 30, 1403 (1969).
[13]M. Freiser, F. Holtzberg, S. Methfessel, G. Pettit, M. Shafer, and J. Suits, Helv. Phys. Acta 41, 832 (1968). The use of optical data to estimate E_i may be somewhat questionable if the final state of the optical transition differs from the conduction band state. However, this value of E_i is consistent with an analysis of the data given in Refs. 2, 4b, 8, and 11.

Enhancement of 3*d* Impurity-Ion Spin-Forbidden Absorption by Color Centers in MgF_2†

L. A. Kappers, S. I. Yun, and W. A. Sibley
Physics Department, Oklahoma State University, Stillwater, Oklahoma 74074
(Received 28 July 1972)

The spin-forbidden optical transitions of Co^{2+}, Ni^{2+}, and Mn^{2+} have been observed in doped crystals of MgF_2 following both γ and electron irradiation. Radiation-induced F centers trapped at impurity sites appear to reduce the forbiddenness significantly for many of the transitions. Oscillator strength increases of up to 10^3 have been recorded.

Over the past decade or so the excellent research of McClure, Ferguson, and their co-workers and others[1-4] has considerably extended our knowledge of the 3*d* impurity-ion transitions in various crystal fields. Unfortunately, these transitions are strongly forbidden and difficult to observe experimentally. In cases of O_h crystal field symmetry many of these transitions are spin and parity forbidden having extremely small oscillator strengths in the range of 10^{-7}. This is a severe limitation since only a few absorption bands can be studied even in relatively thick crystals. High-resolution optical data for more of these transitions would greatly improve our understanding of the spin-orbit coupling, exchange effects, and the interaction of the 3*d* ions with lattice phonons. Therefore, it would be highly desirable to be able to increase the intensity of these strongly forbidden transitions. Recently Sell and Stokowski[5] have hinted at this possibility. They observed in MnF_2 a small increase in the Mn^{2+} absorption induced by the presence of Ca impurities. In this Letter we report that oscillator strengths for Co^{2+}, Ni^{2+}, and Mn^{2+} transitions in MgF_2 can be increased up to 3 orders of magnitude with the aid of radiation-induced color centers. Such large changes also imply that these defect-perturbed transitions might be useful for photochromic devices.[6]

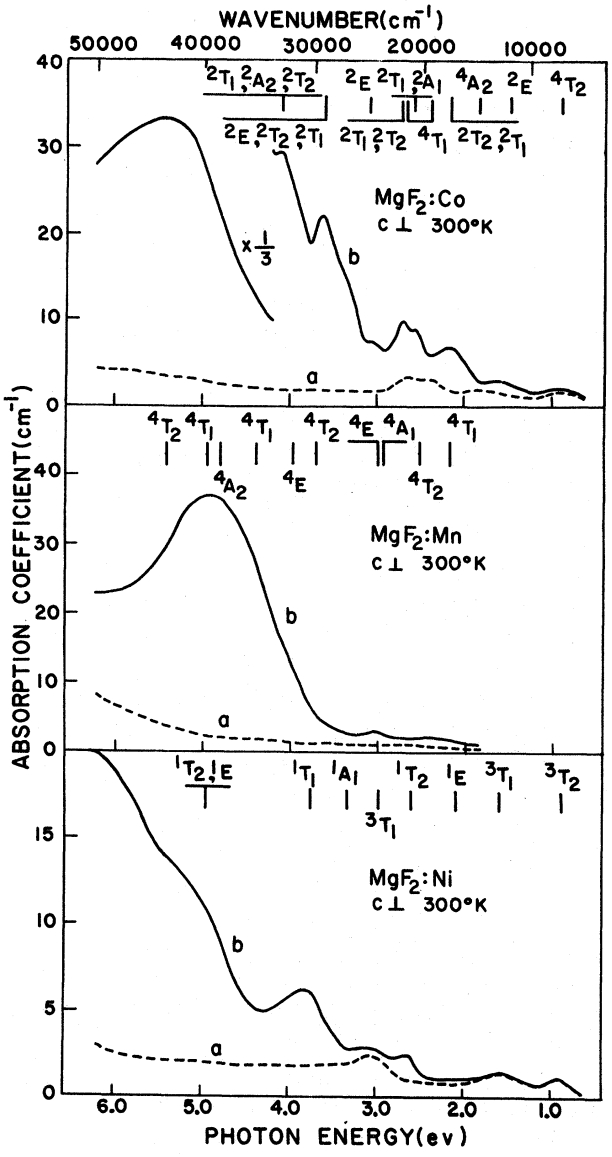

FIG. 1. Room-temperature absorption spectra illustrating the enhancement of the spin-forbidden transitions for Co^{2+}, Ni^{2+}, and Mn^{2+} impurity ions in MgF_2. Spectra labeled *a* represent the absorption in unirradiated crystals while the curves labeled *b* show the absorption following γ irradiation.

TABLE I. Mn^{2+} and Ni^{2+} transitions in MgF_2 crystals.

MgF_2:Mn				MgF_2:Ni			
Assignment (O_h) $^6A_{1g}(^6S) \rightarrow$	Peak Position (cm^{-1})	Oscillator Strength Before Irradiation	Oscillator Strength After Irradiation	Assignment (O_h) $^3A_{2g}(^3F) \rightarrow$	Peak Position (cm^{-1})	Oscillator Strength Before Irradiation	Oscillator Strength After Irradiation
$^4T_{1g}(^4G)$	17 153	3.3×10^{-7}	2.6×10^{-5}	$^3T_{2g}(^3F)$	7 407	6.9×10^{-6}	6.3×10^{-6}
$^4T_{2g}(^4G)$	20 833	2.7×10^{-7}	2.9×10^{-5}	$^3T_{1g}(^3F)$	13 158	8.6×10^{-6}	9.4×10^{-6}
$^4A_{1g}(^4G)$, $^4E_g(^4G)$	24 096	1.9×10^{-7}, 1.1×10^{-7}	1.0×10^{-4}	$^1E_g(^1D)$	16 949	----------	----------
				$^1T_{2g}(^1D)$	21 277	1.8×10^{-7}	8.8×10^{-6}
$^4T_{2g}(^4D)$	29 851	2.0×10^{-7}	1.4×10^{-5}	$^3T_{1g}(^3P)$	24 390	1.9×10^{-5}	1.7×10^{-5}
$^4E_g(^4D)$	31 847	2.9×10^{-7}	2.8×10^{-5}	$^1A_{1g}(^1G)$	27 027	----------	----------
$^4T_{1g}(^4P)$	35 088	3.3×10^{-7}	----------	$^1T_{1g}(^1G)$	30 120	$<4.1 \times 10^{-8}$	3.5×10^{-5}
$^4A_{2g}(^4F)$	38 022	----------	----------	$^1T_{2g}(^1G)$, $^1E_g(^1G)$	40 000	$<3.4 \times 10^{-7}$	1.5×10^{-5}
$^4T_{1g}(^4F)$	40 000	----------	----------				
$^4T_{2g}(^4F)$	43 554	----------	----------				

The $3d$ transition ions have been studied in detail in many different lattices and assignments for the various observed absorption bands have been made. In particular, the observed transitions for Mn^{2+} and Co^{2+} have been assigned in MnF_2,[4,7,8] and those for Ni^{2+} in MgF_2.[3] Since MnF_2 and MgF_2 have the same rutile structure, it is expected that the transitions of the $3d$ impurity ions will be very similar in both hosts. Most investigators have made the approximation that the positive ion site has O_h symmetry in this lattice, although this is not quite the case. The curves labeled *a* in Fig. 1 illustrate the room-temperature absorption for as-grown crystals of MgF_2:Co, MgF_2:Ni, and MgF_2:Mn in the 200- to 2000-nm spectral range. The crystals studied were obtained from Optovac and contain about 2.0 at.% Co, 0.75 at.% Ni, and 0.05 at.% Mn, respectively. These impurity concentrations were used to calculate the oscillator strengths for the observed transitions in curves *a* of Fig. 1. The values are listed in Tables I and II and are very close to those reported previously.[3,7-9]

When MgF_2 crystals are irradiated with electrons or γ rays at room temperature, F centers, negative-ion vacancies each having a trapped electron, are formed. At room temperature these defects are mobile under irradiation and can move through the crystal to form F-aggregate centers or to be trapped adjacent to impurity sites. In the latter case if the impurities are $3d$ transition ions, the optical transitions of these ions can be affected by changes in site symmetry from approximately O_h to C_{4v} and also by exchange between the paramagnetic F-center electron and the $3d$ electrons. It is expected that such interactions would markedly increase the oscillator strengths for these transitions. The curves labeled *b* in Fig. 1 illustrate the optical absorption observed for the doped MgF_2 samples after a (10^7-R) γ irradiation. A dramatic increase of several orders of magnitude in intensity is observed for the previously spin-forbidden transitions as shown by Table I and Table II. However, the spin-allowed transitions, which are observable in the unirradiated crystals, do not increase significantly. This suggests that the dominant effect is due to exchange and that changes in site symmetry do not

TABLE II. Co^{2+} transitions in MgF_2 crystals.

Assignment (O_h) $^4T_{1g}(^4F)\rightarrow$	Peak Position (cm^{-1})	MgF_2:Co Oscillator Strength Before Irradiation	After Irradiation
$^4T_{2g}(^4F)$	7 353	3.0×10^{-6}	3.4×10^{-6}
$^2E_g(^2G)$	11 765	2.5×10^{-8}	1.5×10^{-6}
$^4A_{2g}(^4F)$	14 706	1.6×10^{-6}	1.5×10^{-6}
$^2T_{2g}, ^2T_{1g}(^2G)$	17 331	8.4×10^{-8}	1.0×10^{-5}
$^4T_{1g}(^4P)$	19 231, 21 645	2.1×10^{-5}	2.1×10^{-5}
$^2T_{1g}(^2H)$, $^2A_{1g}(^2G)$	20 534	----------	3.6×10^{-6}
$^2T_{1g}, ^2T_{2g}(^2H)$	21 739	----------	4.8×10^{-6}
$^2E_g(^2H)$	24 938	2.9×10^{-8}	1.5×10^{-6}
$^2T_{1g}(^2P)$, $^2E_g, ^2T_{2g}(^2D)$	29 240	$<6.4 \times 10^{-8}$	3.2×10^{-5}
$^2T_{1g}, ^2A_{2g}(^2F)$, $^2T_{2g}(^2F)$	32 787	$<6.5 \times 10^{-8}$	6.1×10^{-5}

have an appreciable effect on the transitions. Possible assignments for each of the absorption bands are shown in Fig. 1. These tentative assignments were made using the results of previous investigators[3,4,7,10] and the calculations of Liehr.[11]

It is difficult to introduce appreciable amounts of Mn^{2+} into MgF_2. Therefore, since the Mn^{2+} transitions are very weak, it is enlightening to study the excitation spectrum by monitoring the emission from this impurity. Such a spectrum is shown in Fig. 2 and brings out much more detail than the absorption spectrum illustrated in Fig. 1. In fact, the assignments shown on Fig. 1 and in Table I were made from these data. It is interesting to note that the excitation spectrum is almost identical to that[12,13] for Mn^{2+} in $KMgF_3$; however, the luminescence band occurs at a slightly lower energy. The emisstion spectra from MgF_2:Mn are portrayed in the inset of Fig. 2.

In summary, it appears that it is possible with low doses of γ rays or electrons to increase the magnitude of the absorption bands for the 3*d* transition metal ions sufficiently that they can be studied in detail. We realize that the presence of a defect as a nearest neighbor will cause perturbations, but the gain in intensity far outweighs this disadvantage. Another difficulty is the *F*-band absorption which occurs at 260 nm in pure MgF_2 crystals.[14] For these low radiation doses only a small *F* band should be formed, but the possibility of its presence precludes assignments in the uv region. It should be stated that the enhancement of divalent 3*d* impurity ions may be limited to materials such as MgF_2 and $KMgF_3$. Ikeya[15,16] has irradiated NaCl:Mn and found that the radiation changes the valence state of Mn^{2+} to Mn^{1+} and Mn^0. Jain and Lal[17] find similar effects for NaCl:Co. This, of course, would reduce the possibility for this type of investigation in NaCl.

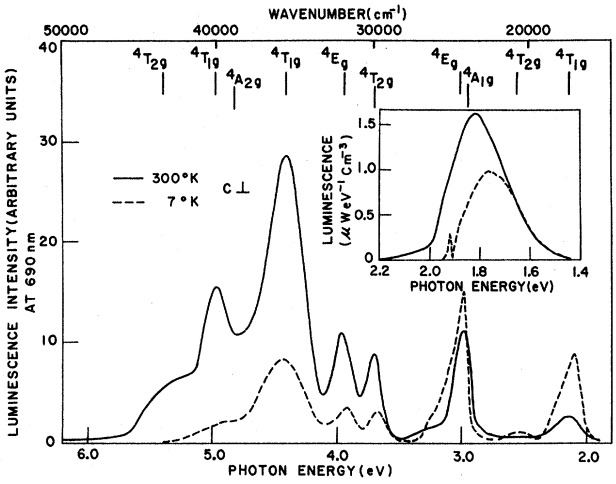

FIG. 2. Excitation spectra of an electron-irradiated MgF_2:Mn crystal at 300 and 7°K. The inset illustrates the emission spectra for Mn^{2+} in the irradiated crystal.

†Work supported by the National Science Foundation Grant No. GP-29545.

[1]D. S. McClure, in *Solid State Physics*, edited by H. Ehrenreich, F. Seitz, and D. Turnbull (Academic Press, New York, 1959), Vol. 9, p. 399.

[2]N. S. Hush and R. J. M. Hobbs, in *Progress in Inorganic Chemistry*, edited by F. A. Cotton (Interscience, New York, 1968), Vol. 10, p. 259.

[3]J. Ferguson, H. J. Guggenheim, H. Kamimura, and Y. Tanabe, J. Chem. Phys. 42, 775 (1965).

[4]J. Ferguson, D. L. Wood, and K. Knox, J. Chem. Phys. 39, 881 (1963).

[5]D. D. Sell and S. E. Stokowski, Phys. Rev. B 3, 2844 (1971).

[6]B. W. Faughnan, D. L. Staebler, and Z. J. Kiss, Appl. Solid State Sci. 2, 107 (1971).

[7]J. W. Stout, J. Chem. Phys. 31, 709 (1959).

[8]R. F. Blunt, J. Chem. Phys. 44, 2317 (1966).
[9]J. Ferguson, H. J. Guggenheim, and D. L. Wood, J. Chem. Phys. 40, 822 (1964).
[10]Y. Tanabe and S. Sugano, J. Phys. Soc. Jap. 9, 753 (1954).
[11]A. D. Liehr, J. Phys. Chem. 67, 1314 (1963).
[12]W. E. Vehse and W. A. Sibley, Phys. Rev. B (to be published).
[13]W. A. Sibley, S. I. Yun, and W. E. Vehse, to be published.
[14]W. A. Sibley and O. E. Facey, Phys. Rev. 174, 1076 (1968).
[15]M. Ikeya and N. Itoh, J. Phys. Soc. Jap. 29, 1295 (1970).
[16]M. Ikeya, Phys. Status Solidi (b) 51, 407 (1972).
[17]S. C. Jain and K. Lal, in *Non-Metallic Crystals*, edited by S. C. Jain and L. T. Chadderton (Gordon and Breach, New York, 1969), p. 219.

New Domain-Wall Configuration for Magnetic Bubbles

A. Rosencwaig, W. J. Tabor, and T. J. Nelson
Bell Laboratories, Murray Hill, New Jersey 07974
(Received 24 July 1972)

A theory based on the hypothesis that the perimeter wall of a magnetic bubble may be composed of alternate Bloch and Néel segments is shown to account quantitatively for the anomalous dependence of diameter on bias field of the recently observed "hard" bubbles in garnet films.

Recently a new class of cylindrical magnetic domains or bubbles has been observed.[1] These new bubbles, designated as hard bubbles, have static and dynamic properties substantially different from those of normal bubbles. Their most anomalous static property is their much larger range of stability in both applied-field and diameter variations. Furthermore any material that allows these hard bubbles also exhibits a range of intermediate bubbles that collapse at fields and diameters intermediate between those of the hard and normal bubbles.

In this Letter we wish to show how the static properties of these hard and intermediate bubbles can be quantitatively explained by assuming the presence of Néel segments in the Bloch wall that forms the perimeter of the bubbles.[2,3]

We therefore consider a hard bubble as having a wall as shown in Fig. 1(a). Here the magnetization is up (+) within the bubble and down (−) outside. The wall itself is composed of a set of Bloch segments of opposing polarity. These Bloch segments are separated from one another by 180° walls which are essentially Néel segments. In Fig. 1(b) we show the central spins through three Bloch segments separated by two Néel segments. We define δ as the width of the Bloch wall, y as the length of a Bloch segment, and x as the length of a Néel segment.

As long as the sense of rotation of the spins around the bubble perimeter is maintained as either clockwise or counterclockwise, then this segmented configuration is frozen in; that is, it is stable against small spin perturbations. If we consider that both the Bloch and Néel segments are walls of uniform rotation,[4] then the wall energy density (energy per unit surface area of the perimeter wall) stored in each segment can be written as

$$\sigma_B = \pi^2 A/\delta + \tfrac{1}{2}K\delta, \qquad (1)$$
$$\sigma_N = \pi^2 A/\delta + \tfrac{1}{2}K\delta + \pi^2 A\delta/2x^2 + \tfrac{1}{2}\pi M^2\delta.$$

Here A is the exchange constant, K the uniaxial anisotropy (with $\frac{1}{2}K$ being the effective anisotropy for spin rotation along the dimension δ),

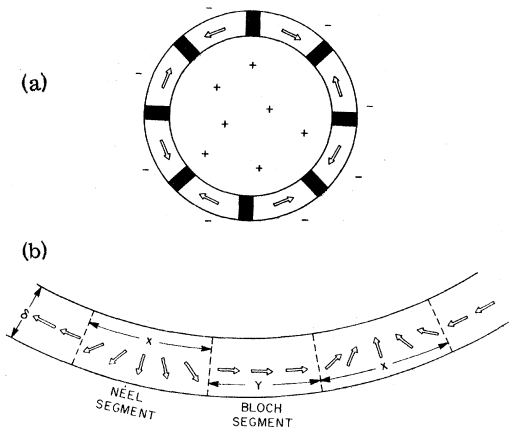

FIG. 1. (a) Top-view representation of a cylindrical magnetic bubble showing the perimeter Bloch wall with Néel segments (dark regions). (b) Representation of the spins in three Bloch wall segments separated by two Néel segments.